Automotive Science and Engineering, Vol. 15, No. 3, (2025), 4784-4795

Iran University of Science and Technology

Automotive Science and Engineering

Journal Homepage: ase.iust.ac.ir

ISSN: 2008-9899

Pareto Optimal Design of a Fuzzy Adaptive Robust Fractional-order PID Controller for an Active Suspension System

M. J. Mahmoodabadi[1*], A. Ansarian[2], T. Zohari[3]

[1]Department of Mechanical Engineering, Sirjan University of Technology, Sirjan, Iran

[2]Department of Electrical and Computer Engineering, Isfahan University of Technology, Isfahan, Iran

[3]Department of Mechanical Engineering, University of Politecnico di Milano, Milan, Italy

ARTICLE INFO

Article history:

Received : 26 Dec 2025

Accepted: 29 Jun 2025

Published: 18 Jul 2025

Keywords:

Fractional-order PID controller

Multi-objective algorithm

Active suspension system

Adaptive robust control

Quarter-car model

Fuzzy system

ABSTRACT

This research proposes a robust fuzzy adaptive fractional-order proportional-integral-derivative (PID) controller for an active suspension system of a quarter-car model. For this, the research first designed the PID controller using chassis acceleration and relative displacement. Next, it utilized the chain derivative rule and the gradient descent mechanism to formulate adaptation rules based on integral sliding surfaces. In the next step, the control parameters were regulated by employing a fuzzy system comprising the product inference engine, singleton fuzzifier, and center average defuzzifier. Eventually, the optimum gains of the proposed controller were determined by running a multi-objective material generation algorithm (MOMGA). Simulation results implied the superiority of the proposed controller over other controllers in handling road irregularities.

1. Introduction

Over the past years, suspension systems (SSs) have become a subject of interest for much research, primarily owing to their potency to deliver thrilling riding, conserve the chassis against road roughness, lessen the unsuitable operations in steering and braking, and improve the stability of the vehicles (Bagheri et al. 2011). All car manufactures comprehend that comfortable driving is a meaningful option for customers. They further know that car body damage emanates from vibrations caused by road bumps. Accordingly, devising versatile SSs has become a central goal for all car manufacturing companies.

The fist SSs developed were passive with a damper and two springs enabling vibrational energy absorption with no need for extra power (Gadhvi et al. 2016). The next generation of such SSs were semi-active, enhancing driving quality and stability by eliminating pitch and roll movements and aftereffect deviations of the braking. These low-frequency systems were available in soft to hard form and could reduce vibrations in the vehicle chassis and body (Ding et al. 2023). And very recently, active SSs have been proposed to synchronize enjoyable driving, comfortable riding, and improved handling. These systems can save, damp, and generate energy by adjusting their features according to motion conditions (Mahmoodabadi and Nejadkourki 2022).

Over the past decades, research has devised diverse control approaches to handle nonlinear SSs (Chen et al. 2025). Of all the control approaches proposed, proportional-integral-derivative (PID) controllers are sought-after by researches and

*Corresponding Author
Email Address: mahmoodabadi@sirjantech.ac.ir
https://doi.org/10.22068/ase.2025.703

industries owing to their simple structure and application. For instance, a PID controller based on a backpropagation neural network is presented in (Jiang and Cheng 2023) for an air SS, where the research reflects the stiffness of rubber bellows. Elsewhere, PID and fuzzy logic controllers are proposed in (Talib et al. 2023) to experimentally investigate ride comfort SSs by running a firefly algorithm. Similarly, ref. (Kumar and Rana 2023) designs a fuzzy PID controller with an electro-hydraulic actuator for nonlinear active SSs, where the cost function is analyzed by fifty runs. A Pareto optimality-based PID controller has been employed in (Gampa et al. 2023) for a vehicle active SS by running the grasshopper optimization algorithm, with the aim of minimizing sprung mass acceleration, tire deflection, and sprung mass suspension deflection. Ref. (Li et al. 2022) devises an improved fuzzy neural network PID controller for an active SS, where body acceleration is pondered as the main optimization target.

Merging fuzzy logic-based systems with controllers can synergistically augment their potency by utilizing human knowledge in the real world. The two key facets reflected by these controllers are insensitivity to environmental factors and robustness. Recent research advocates the efficacy of running fuzzy systems for tuning parameters of control approaches. Some examples are optimal fuzzy PID control (Melese et al. 2025), nonlinear fuzzy PID control (Mohindru 2024), adaptive fuzzy (AF) sliding mode (SM) control (Zheng et al. 2024), self-AF PID control (Abut and Soyguder 2022), fuzzy embedded PID control (Venkataramanan et al. 2024), and AF backstepping control (Liu et al. 2023).

When devising controllers, fractional-order (FO) derivatives and/or integrals can provide the systems with a versatile performance. Oustloup (1988) first suggested applying FO calculus for controllers. Next, Podlobny (1994) introduced a FOPID approach as an illustrious FO controller (Dadras and Momeni 2012). Research has implied the efficiency of merging FO concepts with control schemes. In (Nosheen et al. 2023), FO calculus has been utilized to develop a sensorless speed control aided with an extended Kalman filter for a closed loop induction motor. Ref. (Naderipour et al. 2023) has devised an optimal load-frequency self-tuning FO fuzzy controller for an islanded microgrid to attain robust performance and satisfying flexible structure. An adaptive FOSM disturbance observer (DO)-based robust theoretical frequency controller has been utilized in (Guha et al. 2023) for a hybrid wind–diesel power system to minimize chattering in the control effort and attain promoted robustness against external disturbances. Ref. (Liu et al. 2023) has employed a FO controller based on digital-twin-based real-time optimization for industrial robots modeled in a digital environment to realize all-around 3D visual monitoring and strong interactive. Elsewhere, ref. (Ansarian and Mahmoodabadi 2023) reports a Fuzzy Adaptive (FA) robust FOPID controller optimized by a MO approach for a nonlinear unmanned flying system, where the fuzzy systems employ the product inference engine, center average defuzzifier, singleton fuzzifier, and triangular-trapezoidal membership functions.

In real applications of controller design, balancing output errors and control efforts is paramount. Metaheuristic (MH) algorithms mostly utilized to optimize MO problems have recently been sought-after by researchers (Peng et al. 2025). Research implies the potency of these algorithms in solving MO control problems. Ref. (Wang et al. 2023) reports a MO approach for a hydrogen-fueled rotary engine based on GA and machine learning (ML). Ref. (Tamashiro et al. 2023) employs an optimal components capacity based MO scheme and an optimal scheduling-based MPC optimization algorithm for smart apartment buildings. In (Zhou et al. 2023), an adaptive adjustment inertia weight particle swarm optimization (PSO) algorithm has been run used for the optimal design of a cable-driven parallel robot. Ref. (Abedzadeh Maafi et al. 2021) uses an MOGA for the optimal design of a FA hierarchical SM controller of an XZ inverted pendulum system. Ref. (Kapnopoulos et al. 2022) uses a cooperative PSO strategy containing position and attitude control parameters for gain tuning of an MPC-based quadrotor trajectory tracking scheme.

To enhance the breadth of recent advancements, this study also considers the following contributions:

•Multi-criteria suspension optimization (Gheibollahi and Masih-Tehrani 2023)

•Fuzzy Sliding mode control in vehicle dynamics (Najafi et al. 2023)

•Genetic algorithms for vehicle design (Gheibollahi et al. 2024)

•Stability under varying road conditions (Damavandi et al. 2022)

•Semi-active suspension energy efficiency (Nazemian and Masih-Tehrani 2020)

•ISO-based road roughness modeling (Nazemian and Masih-Tehrani 2020)

•Vehicle dynamics under uncertainty (Nazemi et al. 2022)

•Recent H∞-based suspension control schemes (Damavandi et al. 2025)

[DOI: 10.22068/ase.2025.703]

•Robustness in suspension design (Najafi and Masih-Tehrani 2022).

Contrary to (Bagheri et al. 2011, Ding et al. 2023) applying passive and semi-active SSs, the present research proposes a hybrid controller by merging FOPID compensators, sliding surfaces, and fuzzy systems. This controller aims to stabilize a nonlinear active SS. Hence, this research devises a PID controller improved by FO concepts to handle the nonlinear dynamics in the concerned active SS. The sliding surfaces are calculated via the system states to adapt the gains of the FOPID controller according to the system conditions. This research employs a fuzzy system based on the center average defuzzifier, singleton fuzzifier, and product inference engine to regulate the sliding surface parameters. Contrary to (Talib et al. 2023, Kumar and Rana 2023) that employ single objective optimization, this research (after designing the structure of the proposed control system) uses the MO material generation algorithm (MOMGA) to determine the optimal values of the adaptation coefficients, fuzzy system parameters, and fractional orders. The aim is to coincidently minimize body acceleration and relative displacement. Eventually, simulation results are depicted to illustrate the potency of the proposed method in handling the concerned active SS compared to other controllers.

The remaining sections are organized as follows. Section 2 discusses the dynamical formulations of the active SS. Section 3 explain adaptive FOPID controllers and fuzzy systems. Section 4, runs the MOMGA to define the appropriate values of the design coefficients. Section 5 presents the simulation results to show the superiority of the proposed method over recently introduced methods. Ultimately, Section 5 concludes the results and offers prospects.

2. Dynamical Equations

The dynamical equations of the active SS shown in Figure 1 can be written as follows (Mahmoodabadi and Nejadkourki 2022).

$$m_r\ddot{z}_r(t) + c_s[\dot{z}_r(t) - \dot{z}_s] + k_s[z_r(t) - z_s(t)] + k_r[z_r(t) - z_w(t)] = -\tau(t) \quad (1)$$

$$m_s\ddot{z}_s(t) + c_s[\dot{z}_s(t) - \dot{z}_r] + k_s[z_s(t) - z_s(t)] = \tau(t) \quad (2)$$

where $\tau(t)$ denotes the control effort. $z_r(t)$ and $z_s(t)$ are, respectively, the vertical displacement of the tire and sprung mass, $\dot{z}_r(t)$ and $\dot{z}_s(t)$ denote their vertical velocities, and $\ddot{z}_r(t)$ and $\ddot{z}_s(t)$ represent their vertical acceleration. In addition, m_r, m_s, c_s, k_s, and k_r define the tire mass, sprung mass, damping coefficient, spring stiffness coefficient, and tire stiffness coefficient, correspondingly. Ultimately, $z_w(t)$ indicates the vertical displacement caused by irregularities that can be formulated as follows.

$$z_w(t) = \begin{cases} 0.05[\sin(2\pi t)] & if\ 0.5<t<2.5 \\ 0 & else \end{cases} \quad (3)$$

In this study, a deterministic road input defined by Equation (3) is used to evaluate the baseline performance of the proposed controller. Although more realistic stochastic road profiles can be generated based on ISO 8608 standards, they were not considered in this initial model to isolate the controller's performance under controlled conditions. Incorporating ISO-compliant random road excitations is proposed as a direction for future work.

It is also worth noting that the employed quarter-car model only captures vertical dynamics. Hence, the effects of lateral load transfer and roll dynamics during cornering maneuvers are not reflected in the current formulation. Extension to a half-car or full-vehicle model would be necessary to account for such phenomena in future studies.

Table 1. Values of the constant coefficients for the studied vehicle SS according to Ref. (Mahmoodabadi and Nejadkourki 2022) .

coefficient	value	unit
m_r	36	kg
m_s	240	kg
c_s	1978	kNs/m
k_r	160000	kN/m
k_s	10529	kN/m

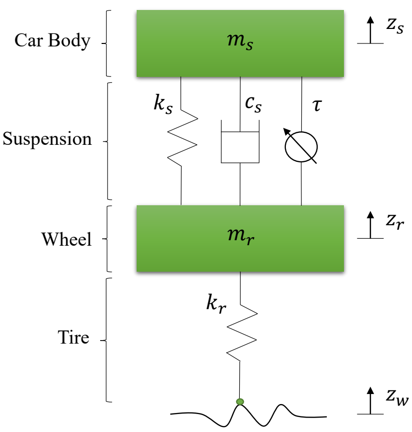

Figure 1: A schematic representation of the studied quarter-car active SS.

Table 1 tabulates the numerical values of the constant parameters in Equations (1) and (2) and

[DOI: 10.22068/ase.2025.703]

compares these results with those reported in Ref. (Mahmoodabadi and Nejadkourki 2022).

3. Controller Design

3.1. Fractional-order PID Controller

The PID, as a widely known controller, is extensively employed owing to its efficacy and simplicity (Aessa et al. 2023). Recently, response speed and robustness have been reported in the FO version of this compensator (El-Rifaie et al. 2025, Sahin et al. 2024). Some definitions of the FO operators are described in the following (Ansarian and Mahmoodabadi 2023).

Definition 1. Caputo fractional of λ^{th} order derivative and integral for function $k_{(t)}$ are given by the following equations.

$$ {}_{t_0}^{c}D_t^{\lambda}k(t) = \frac{1}{\mathrm{H}(\lambda-\gamma)}\int_{t_0}^{t}\frac{k^{(\gamma)}(\tau)}{(t-\tau)^{\lambda-\gamma+1}}d\tau \tag{4}$$

$$ {}_{t_0}^{c}I_t^{\lambda}k(t) = \frac{1}{\mathrm{H}(\lambda)}\int_{t_0}^{t}\frac{k(\tau)}{(t-\tau)^{1-\lambda}}d\tau \tag{5}$$

where $\gamma - 1 < \lambda \leq \gamma$, and γ represents the smallest integer number greater than λ. Further, t and t_0 are the final and initial time values, respectively reflecting the upper and lower bounds of integration. $\mathrm{H}(.)$ denotes the Gamma function written by the following equation.

$$\mathrm{H}(\omega) = \int_0^{\infty} e^{-t}\, t^{\omega-1}dt \tag{6}$$

Therefore, a common version of the FOPID controller for a system with two errors e_1 and e_2 can be revealed as follows.

$$\tau(t) = \tilde{\eta}_{p1}e_1(t) + \tilde{\eta}_{i1}I^{\nu}e_1(t) + \tilde{\eta}_{d1}D^{\rho}e_1(t) + \tilde{\eta}_{p2}e_2(t) + \tilde{\eta}_{i2}I^{\nu}e_2(t) + \tilde{\eta}_{d2}D^{\rho}e_2(t) \tag{7}$$

where $\tilde{\eta}_{p1}$, $\tilde{\eta}_{i1}$, $\tilde{\eta}_{d1}$ and $\tilde{\eta}_{p2}$, $\tilde{\eta}_{i2}$, $\tilde{\eta}_{d2}$ are proportional, integral, and derivative coefficients related to the first and second errors, respectively. Correspondingly, D^{ρ} and I^{ν} are Caputo fractional derivative and integral of orders ρ and ν.

3.2. Adaptive Robust Fractional-order PID controller

When designing a controller, a key aspect is to attain appropriate values for the control gains. For this, adaptive methods are supposedly highly potent to timely set these gains. Furthermore, robust SM techniques can be utilized to modify time-dependent relations of the adaptive approach. Thus, integral sliding surfaces related to a system with two errors can be calculated from the equation below (Slotine and Li 1991).

$$s_j = e_j + \tilde{c}_j \int e_j\, dt, \quad j = 1,2 \tag{8}$$

where e_j $j = 1,2$ denotes the system errors based on the system states, and $\tilde{c}_j$ $j = 1,2$ represent sliding surface parameters that can be obtained from the equation below.

$$\tilde{c}_j = \hat{c}_j + c_j, \quad j = 1,2 \tag{9}$$

where, c_j $j = 1,2$ are positive constant parameters, while $\tilde{c}_j$ $j = 1,2$ signify fuzzy parameters. The time-dependent adaptive part of the proportional, integral, and derivative coefficients can be calculated utilizing the gradient descent technique as follows (Astrom and Wittenmark 2008).

$$\dot{\bar{\eta}}_{pj} = -\tilde{\alpha}_{pj}s_j e_j, \quad j = 1,2 \tag{10}$$

$$\dot{\bar{\eta}}_{ij} = -\tilde{\alpha}_{ij}s_j \int e_j\, dt, \quad j = 1,2 \tag{11}$$

$$\dot{\bar{\eta}}_{dj} = -\tilde{\alpha}_{dj}s_j \frac{de_j}{dt}, \quad j = 1,2 \tag{12}$$

where, $\tilde{\alpha}_{pj}$, $\tilde{\alpha}_{ij}$ and $\tilde{\alpha}_{dj}$ can be regulated by fuzzy parameters $\hat{\alpha}_{pj}$, $\hat{\alpha}_{ij}$ and $\hat{\alpha}_{dj}$, respectively.

$$\tilde{\alpha}_{xj} = \hat{\alpha}_{xj} + \alpha_{xj}, \; j = 1,2, x = p, i, d \tag{13}$$

where, α_{xj} $j = 1,2$ and $x = p, i, d$ denote positive constant parameters. Ultimately, the coefficients of the FOPID controller introduced in Equation (7) can be clarified as follows.

$$\tilde{\eta}_{xj} = \eta_{xj} + \bar{\eta}_{xj} \quad j = 1,2 \; and \; x = p, i, d \tag{14}$$

where, η_{xj} $j = 1,2$ and $x = p, i, d$ indicate positive constant parameters..

3.3. Fuzzy adaptive robust fractional-order PID controller

In the previous subsection, a series of parameters arose when adapting the FOPID control gains. Hence, one potent solution to regulate their values based on the system conditions is to apply fuzzy logic-based systems. As with Equations (10-12), the sliding surfaces influence the overall behavior of the control approach. Therefore, regulating their parameters can affect the system's performance. This research employs fuzzy systems to regulate positive control parameters $\hat{c}_j$ $(j = 1,2)$ and $\hat{\alpha}_{xj}$ $(j = 1,2 \; and \; x = p, i, d)$. The studied fuzzy systems employ the product inference engine, singleton fuzzifier, and center average defuzzifier, which are formulated as follows (Driankov et al. 2013).

$$\text{fuzzy parameter} = \frac{\sum_{k=1}^{N}\bar{f}^{k}(\mu^{k}(e_k))}{\sum_{k=1}^{N}(\mu^{k}(e_k))} \tag{15}$$

where N_1 and N_2 are the numbers of the fuzzy rules and equal to 3, and $\bar{f}^{k_1 k_2}$ represents the center of

[DOI: 10.22068/ase.2025.703]

the output membership functions. Ultimately, μ^k denotes the input membership function that is pondered as a triangular shape (Figure 2). Furthermore, the fuzzy rules related to the control parameters are given in Table 2.

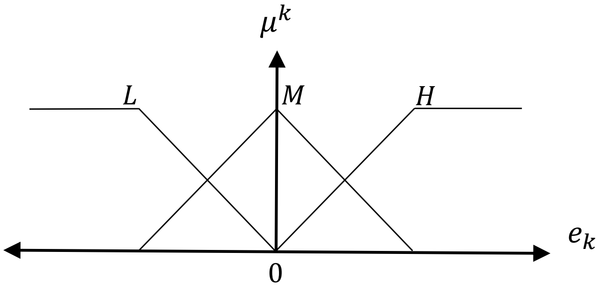

Figure 2. Triangular membership functions utilized for the inputs of the fuzzy systems.

Table 2. Fuzzy rules for fuzzy parameters $\bar{f}^k$.

	L	M	H
$\hat{c}_1$	96.04	49.98	96.04
$\hat{c}_2$	18876	229	13.44
$\hat{\alpha}_{p1}$	1489	6157	2401
$\hat{\alpha}_{i1}$	67110	978	984
$\hat{\alpha}_{d1}$	5497	1520	3326
$\hat{\alpha}_{p2}$	24990	1092	17767
$\hat{\alpha}_{i2}$	834.5	20.99	201.6
$\hat{\alpha}_{d2}$	0.099	0.014	0.093

4. Optimization by the MOMGA

Over the last decades, MH algorithms have become popular due to their simplicity, flexibility, derivation-free mechanism, and local optima avoidance (Sadeghian et al. 2025). These features qualify MH optimization approaches as potent solves of the real-world issues, particularly controller design problems (Zhuang et al. 2024). David Schaffer proposed the theory of MO optimization for problems with diverse and potentially conflicting objectives (Schaffer and Grefenstette 1985). Hence, a MO optimization technique based on the material generation algorithm (MGA) can find the optimum values of control gains.

4.1. MGA

Inspired by the configuration of chemical reactions and compounds in producing new materials, the MGA offers highly competitive and even eminent results compared to other MH algorithms (Talatahari et al. 2021). Alike natural evolution algorithms that build a predefined population of solution candidates, MGA determines a number of materials (MT), comprised of multiple periodic table elements (Es). A general mathematical modeling of this algorithm is as follows (Talatahari et al. 2021).

$$MT = \begin{bmatrix} E_1^1 & E_1^2 & \cdots & E_1^i & \cdots & E_1^b \\ E_2^1 & E_2^2 & \cdots & E_2^j & \cdots & E_2^b \\ \vdots & \vdots & & \vdots & & \vdots \\ E_j^1 & E_j^2 & \cdots & E_j^i & \cdots & E_j^b \\ \vdots & \vdots & & \vdots & & \vdots \\ E_m^1 & E_m^1 & \cdots & E_m^i & \cdots & E_m^b \end{bmatrix} \quad (16)$$

$$E_j^i(0) = E_{j,min}^i + urand(0,1)\,(E_{j,max}^i - E_{j,min}^i) \quad (17)$$

$$MT_{new} = [E_{new}^1 \quad E_{new}^2 \quad \cdots \quad E_{new}^s \quad \cdots \quad E_{new}^b] \quad (18)$$

$$E_{new}^s = E_{r_1}^{r_2} \pm pc \quad (19)$$

$$f(E_{new}^s|\mu,\sigma^2) = \frac{1}{\sqrt{2\pi\sigma^2}}\; e^{\frac{-(x-\mu)^2}{2\sigma^2}} \quad (20)$$

where b is the dimension of the problem, m is the total number of solution candidates, $E_j^i(0)$ denotes the initial amount of the ith periodic table element in the jth material, $urand\ (0,1)$ signifies a random number uniformly distributed between [0,1], $E_{j,min}^i$ and $E_{j,max}^i$ respectively indicate the minimum and maximum acceptable amounts of the ith decision variable in the jth solution candidate, r_1 and r_2 correspondingly denote random integers uniformly spread in $[1, m]$ and $[1, b]$, $PT_{r_1}^{r_2}$ (randomly chosen from the MT, MT_{new}) represents the new generated material, PT_{new}^s is the new periodic table element, and pc is the probabilistic component regulating the process of gaining, losing, or even sharing electrons.

4.2. MOMGA

MGA was originally introduced to address single-objective optimization problems and cannot be directly used to solve MO issues. MGA, in turn, requires three mechanisms for solving MO optimization problems. The first mechanism is the archive, a storage space for storing or restoring the obtained Pareto optimal solutions. The second effective approach to enhance non-dominated solutions in the archive is the grid mechanism. When the archive is full, the grid mechanism rearranges the object space's segmentation and finds the most populated zone to prune it. The leader mechanism is the last method introduced to the MGA, which is used to compare solutions in the MO search space. Such a selection is based on the roulette-wheel technique with the following probability:

$$T_i = \frac{p}{n_i} \quad (21)$$

where p is a constant number higher than 1, and n_i denotes the variety of obtained Pareto optimal solutions in the ith section (Nouhi et al. 2022). The MOMGA flowchart is illustrated in Figure 3.

[DOI: 10.22068/ase.2025.703]

Ultimately, the block diagram of the optimal FA robust FOPID controller is demonstrated in Figure 4.

5. Simulation results and discussion

The MOMGA was utilized to find the best values for control parameters, including the positive constant parameters in Equations (9), (13), and (14), the initial conditions for the adaptive gains in Equations (10) through (12), the FO operators in Equation (7), and the centers of the output membership functions in Equation (15). The controller optimization process was formulated as a multi-objective problem with two primary objectives:

(1) Minimization of the integral of absolute relative displacement

$$f_1 = \int |z_s - z_r|\, dt \tag{22}$$

which reflects road holding performance, and

(2) Minimization of the integral of absolute chassis acceleration

$$f_2 = \int |\ddot{z}_s|\, dt \tag{23}$$

which is directly related to ride comfort in accordance with ISO 2631 guidelines. These two criteria represent the widely accepted trade-off in suspension design, ensuring both stability and passenger comfort.

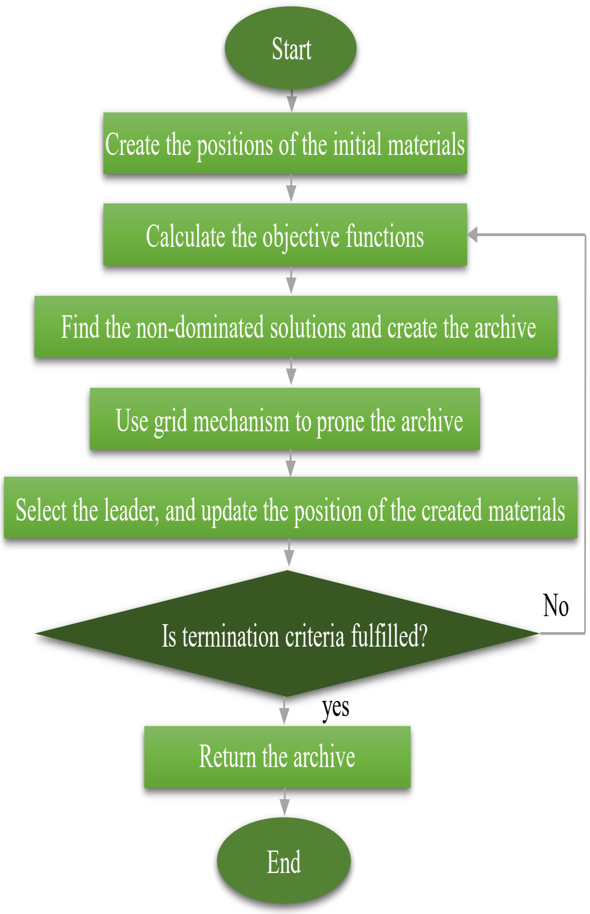

Figure 3. Flowchart of the MOMGA.

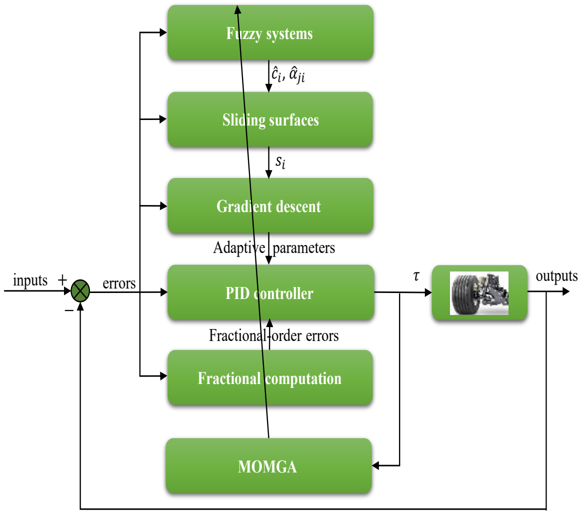

Figure 4. Block diagram of the introduced optimal fuzzy adaptive robust fractional-order PID controller.

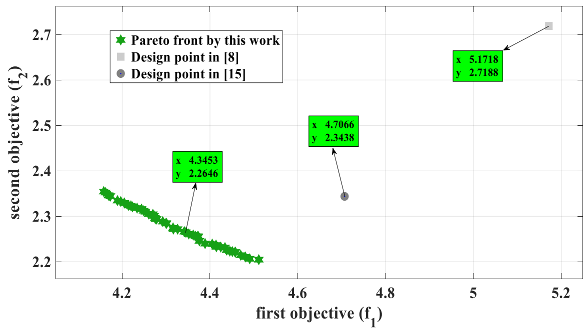

Figure 5. Pareto front as well as the design points obtained by this strategy and suggested in (Bagheri et al. 2011, Mahmoodabadi and Nejadkourki 2022).

Figure 5 depicts the Pareto front achieved through the optimization process and the chosen point, and compares them with the optimum points in (Bagheri et al. 2011, Mahmoodabadi and Nejadkourki 2022). Ref. (Bagheri et al. 2011) has used the MOMGA for Pareto optimization of the two-degree-of-freedom passive linear SS regarding these two conflicting functions. Likewise, Ref. (Mahmoodabadi and Nejadkourki 2022) has designed an FA robust PID controller optimized by a single-objective PSO algorithm for the quarter-car model with an active SS.

To fairly compare these results with those in (Rodriguez-Guevara et al. 2023, Bagheri et al. 2011), the values of the constant parameters for the concerned vehicle SS are reflected based on the data in Table 1 for all methods. Compared to the solutions related to the designed points proposed in (Bagheri et al. 2011, Mahmoodabadi and Nejadkourki 2022), the chosen point from the

[DOI: 10.22068/ase.2025.703]

Pareto front has been improved by 8% and 19% (in the relative displacement) and by 3% and 20% (in the chassis acceleration), respectively. Such improvements enhance both road holding and ride comfort, and the resulting chassis acceleration levels fall within ISO 2631 comfort thresholds for light vehicles. Table 3 presents the optimum values of the defined variables, including the initial values of the adaptive coefficients, the FO parameters, and the constant parameters of the gradient descent formulations. Figures 6 and 7 depict the time responses of relative displacement and the chassis acceleration, respectively. As shown, the proposed approach has less relative displacement and has been improved by 27% and 104% (in the overshoot values) and by 5% and 45% (in the settling time values), compared to the methods designed in (Bagheri et al. 2011, Mahmoodabadi and Nejadkourki 2022). Figures 8 to 11 show displacements and velocities of the tire and chassis for the different methods. As demonstrated, the proposed optimal FA robust FOPID control system takes less overshot values and more efficiently suppresses vehicle vibrations, compared to the control approaches in (Bagheri et al. 2011, Mahmoodabadi and Nejadkourki 2022). The results indicate that the proposed FA robust FOPID controller effectively suppresses oscillations in both sprung and unsprung masses. Although the optimization emphasizes ride comfort, the achieved improvements do not significantly compromise the response time or overshoot. This balance reflects the inherent trade-off in suspension design and highlights the controller's effectiveness in tuning fractional gains adaptively. Figure 12 shows the behaviors of the sliding surfaces without chattering and acceptable ranges. Ultimately, Figures 13 and 14 respectively show variations in the fuzzy and adaptive gains related to the proportional, integral, and derivative terms over time. These diagrams imply the convergence of all parameters to constant values at a reasonable period. It should be noted that the quarter-car model employed in this study does not capture lateral dynamics such as roll or yaw, which are relevant during cornering maneuvers. Therefore, the current analysis is limited to vertical excitations. Future research should extend the model to half-car or full-car configurations to enable comprehensive validation under combined vertical and lateral scenarios.

To evaluate the robustness of the controller against parameter variations, a sensitivity analysis was conducted. The sprung mass was varied within ±10% of its nominal value as reported in Table 1. This range reflects common tolerances observed in practical applications and component variability. The system's performance under this uncertainty illustrated in Figure 15 was used to assess the controller's robustness in terms of stability and comfort.

Table 3. Optimum values of the control parameters according to the suggested design point.

Variable	Value	Variable	Value
c_1	67626	η_{i2}	19.95
c_2	416.16	η_{d2}	0.480
α_{p1}	388.96	$\bar{\eta}_{p1}(0)$	3128.98
α_{i1}	4.99	$\bar{\eta}_{i1}(0)$	3043.50
α_{d1}	125.94	$\bar{\eta}_{d1}(0)$	3164.80
α_{p2}	0.960	$\bar{\eta}_{p2}(0)$	48.99
α_{i2}	2.895	$\bar{\eta}_{i2}(0)$	503.54
α_{d2}	9.996	$\bar{\eta}_{d2}(0)$	0.007
η_{p1}	416.16	ν	0.916
η_{i1}	496.57	ρ	1.163
η_{d1}	499.80	η_{p2}	145.65

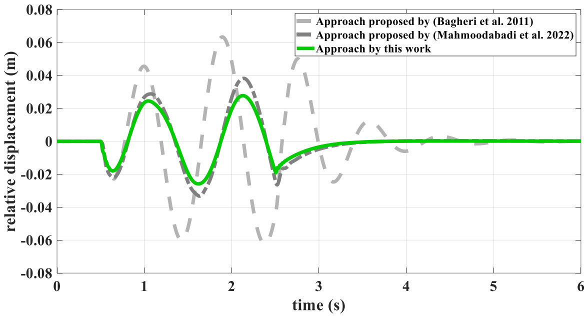

Figure 6. Time changes of the relative displacement.

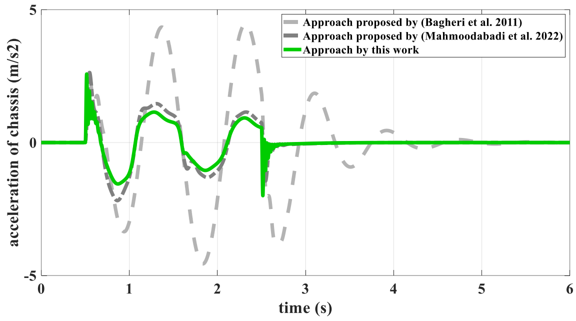

Figure 7. Time changes of the acceleration of chassis.

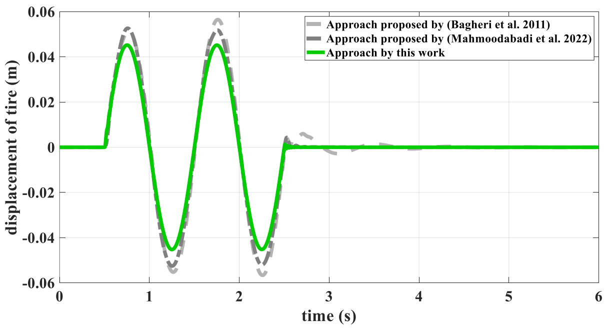

Figure 8. Time changes of the displacement of tire.

[DOI: 10.22068/ase.2025.703]

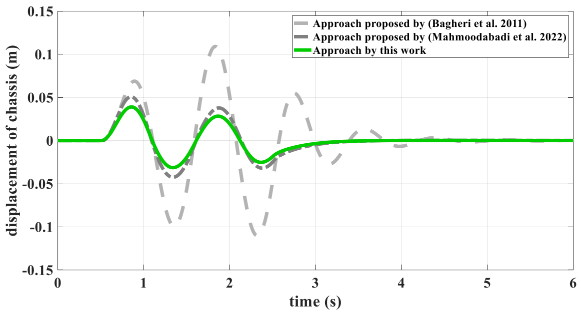

Figure 9. Time changes of the displacement of chassis.

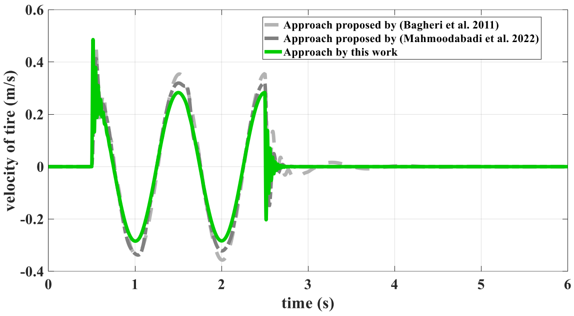

Figure 10. Time changes of the velocity of tire.

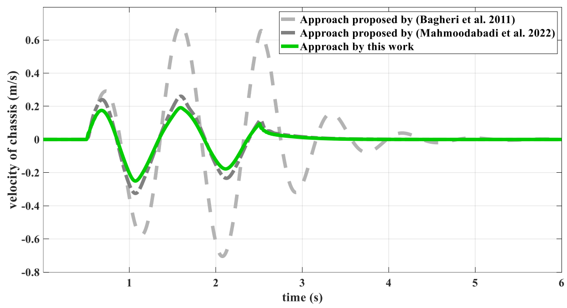

Figure 11. Time changes of the velocity of chassis.

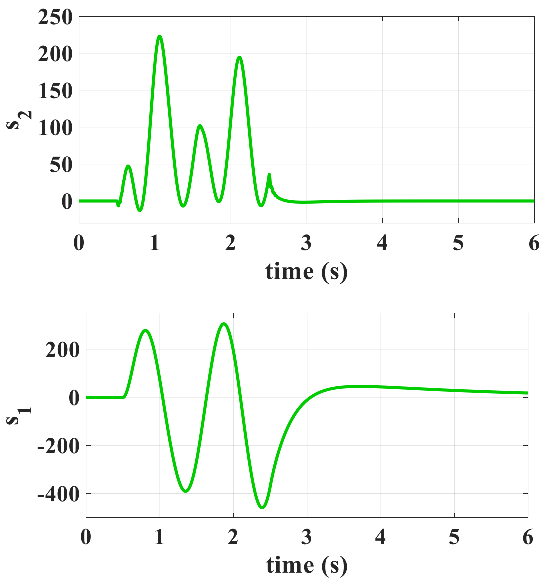

Figure 12. Time variations of the sliding surfaces for the proposed method of this work.

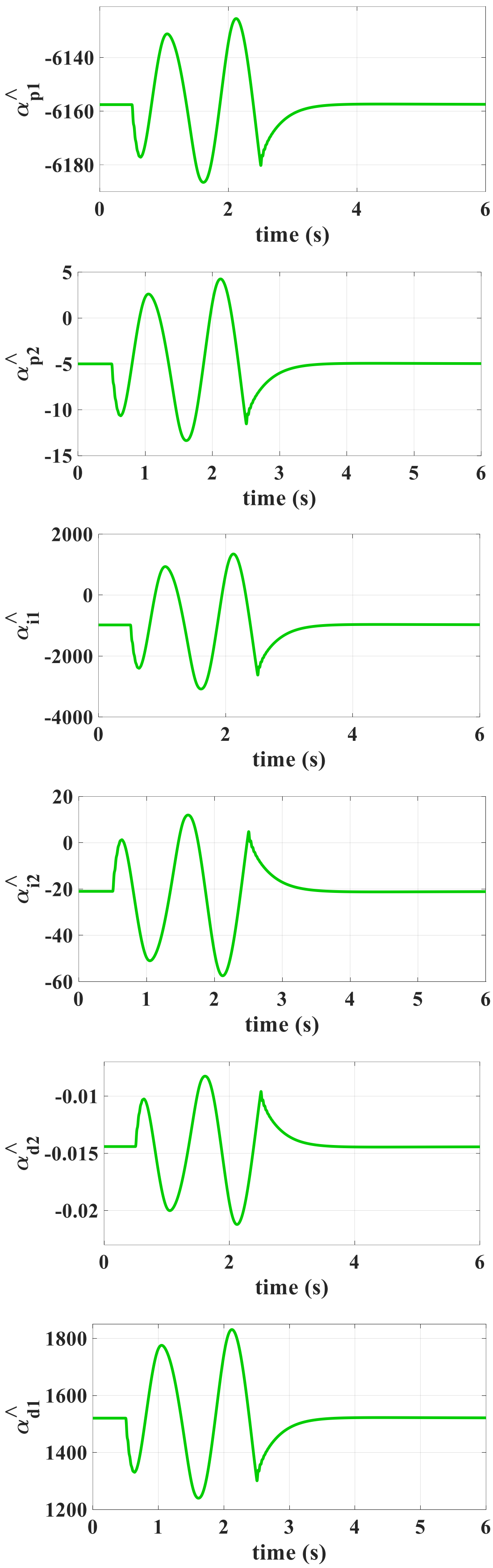

Figure 13. Time variation of the fuzzy gains for the proposed method of this work.

[DOI: 10.22068/ase.2025.703]

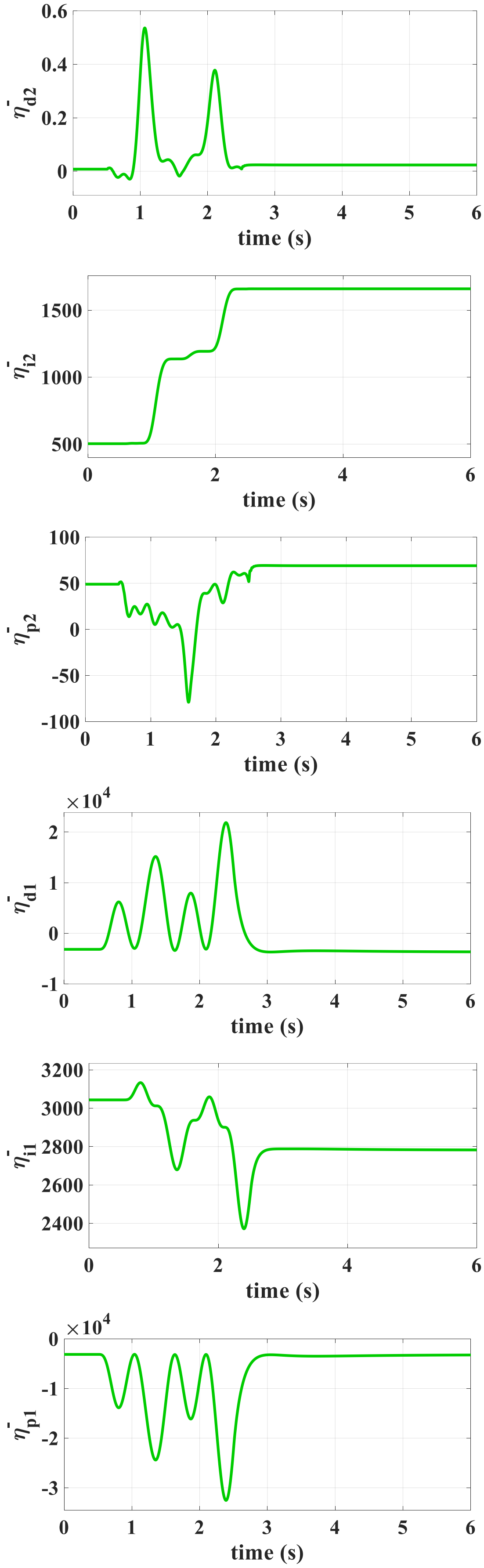

Figure 14. Time responses of the adaptive gains for the proposed method of this work.

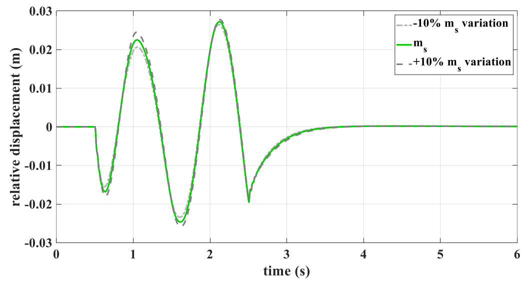

Figure 15. Time changes of the relative displacement over ±10% m_s variation.

6. Conclusions and Future Works

This research proposed a hybrid controller constituting FOPID compensators, sliding surfaces, and fuzzy systems for an active SS. Firstly, a PID controller improved by the FO concepts was proposed to handle the dynamics of the studied nonlinear active SS. Next, the sliding surfaces were formulated based on the relative displacement and chassis acceleration to adaptively compute the gains of the FOPID controller. Then, Fuzzy systems based on the center average defuzzifier, singleton fuzzifier, and product inference engine were used to regulate the parameters of the sliding surfaces and gradient descent equation. After the control system was structurally designed, the MOMGA was run to determine the optimal values of the constant gains, aiming to simultaneously minimize body acceleration and relative displacement. Simulation results revealed the potency of the propose idea in handling vibrations in the active SS, compared to ot her controllers. Regarding these, future research needs to (1) apply other novel MOMGAs to obtain more accurate non-dominate solutions, (2) utilize more complete models of the vibration system to achieve more pragmatic results, and (3) employ other fuzzy systems (e.g., Takagi-Sugeno and fuzzy type II systems)

to enhance the flexibility of the controller design process.

References

Bagheri A, Mahmoodabadi MJ, Rostami H, and Kheybari S (2011) Pareto optimization of a two-degree of freedom passive linear suspension using a new multi-objective genetic algorithm.

Gadhvi B, Savsani V, and Patel V (2016) Multi-objective optimization of vehicle passive suspension system using NSGA-II, SPEA2 and PESA-II. Procedia Technology, 23, 361-368.

[DOI: 10.22068/ase.2025.703]

Ding R, Wang R, Meng X, and Chen L (2023) Research on time-delay-dependent H∞/H2 optimal control of magnetorheological semi-active suspension with response delay. Journal of Vibration and Control, 29(5-6), 1447-1458.

Mahmoodabadi MJ, and Nejadkourki N (2022) Optimal fuzzy adaptive robust PID control for an active suspension system. Australian Journal of Mechanical Engineering 20(3), 681-691.

Chen L, Xu X, Liang C, Jiang XW, and Wang F (2023) Semi-active control of a new quasi-zero stiffness air suspension for commercial vehicles based on H2H∞ state feedback. Journal of Vibration and Control 29(7-8), 1910-1926.

Jiang X, and Cheng T (2023) Design of a BP neural network PID controller for an air suspension system by considering the stiffness of rubber bellows. Alexandria Engineering Journal 74, 65-78.

Ab Talib MH, Mat Darus IZ, Mohd Samin P, Mohd Yatim H, Hadi MS, Shaharuddin NMR, and Mohd Yamin AH (2023) Experimental evaluation of ride comfort performance for suspension system using PID and fuzzy logic controllers by advanced firefly algorithm. Journal of the Brazilian Society of Mechanical Sciences and Engineering 45(3), 132.

Kumar V, and Rana KPS (2023) A novel fuzzy PID controller for nonlinear active suspension system with an electro-hydraulic actuator. Journal of the Brazilian Society of Mechanical Sciences and Engineering 45(4), 189.

Gampa SR, Mangipudi SK, Jasthi K, Goli P, Das D, and Balas VE (2022) Pareto optimality based PID controller design for vehicle active suspension system using grasshopper optimization algorithm. Journal of Electrical Systems and Information Technology 9(1), 24.

Li M, Li J, Li G, and Xu J (2022) Analysis of active suspension control based on improved fuzzy neural network PID. World Electric Vehicle Journal 13(12), 226.

Melese YL, Alitasb GK, and Belete MD (2025) Optimal fuzzy-PID controller design for object tracking. Scientific Reports 15(1), 12064.

Mohindru P (2024) Review on PID, fuzzy and hybrid fuzzy PID controllers for controlling non-linear dynamic behaviour of chemical plants. Artificial Intelligence Review 57(4), 97.

Zheng Y, Zheng J, Shao K, Zhao H, Man Z, and Sun Z (2024) Adaptive fuzzy sliding mode control of uncertain nonholonomic wheeled mobile robot with external disturbance and actuator saturation. Information Sciences 663, 120303.

Abut T, and Soyguder S (2022) Two-loop controller design and implementations for an inverted pendulum system with optimal self-adaptive fuzzy-proportional–integral–derivative control. Transactions of the Institute of Measurement and Control 44(2), 468-483.

Venkataramanan K, Arun M, Jha S, and Sharma A (2024) RETRACTED: Analyzing stability and structural aspects of embedded fuzzy type 2 PID controller for robot manipulators. Journal of Intelligent & Fuzzy Systems, 46(1), 1429-1442.

Liu W, Cheng X, and Zhang J (2023) Command filter-based adaptive fuzzy integral backstepping control for quadrotor UAV with input saturation. Journal of the Franklin Institute 360(1), 484-507.

Dadras S, and Momeni HR (2012) Fractional terminal sliding mode control design for a class of dynamical systems with uncertainty. Communications in Nonlinear Science and Numerical Simulation 17(1), 367-377.

Nosheen T, Ali A, Chaudhry MU, Nazarenko D, Shaikh IUH, Bolshev V, and Panchenko V (2023) A fractional order controller for sensorless speed control of an induction motor. Energies 16(4), 1901.

Naderipour A, Abdul-Malek Z, Davoodkhani IF, Kamyab H, and Ali RR (2023) Load-frequency control in an islanded microgrid PV/WT/FC/ESS using an optimal self-tuning fractional-order fuzzy controller. Environmental Science and Pollution Research 30(28), 71677-71688.

Guha D, Roy PK, and Banerjee S (2023) Adaptive fractional-order sliding-mode disturbance observer-based robust theoretical frequency controller applied to hybrid wind–diesel power system. ISA transactions 133, 160-183.

Liu X, Gan H, Luo Y, Chen Y, and Gao L (2023) Digital-twin-based real-time optimization for a fractional order controller for industrial robots. Fractal and Fractional 7(2), 167.

Ansarian A, and Mahmoodabadi MJ (2023) Multi-objective optimal design of a fuzzy adaptive robust fractional-order PID controller for a nonlinear unmanned flying system. Aerospace Science and Technology 141, 108541.

Peng Z, Huang J, Lv J, Ye J (2025) Multi-objective optimization of cold plate with spoiler for battery thermal management system using whale optimization algorithm. Applied Thermal Engineering 260, 124974.

Schaffer JD, and Grefenstette JJ (1985) Multi-Objective Learning via Genetic Algorithms. In Ijcai 85, 593-595.

Zhuang X, Wang W, Su Y, Yan B, Li Y, Li L, and Hao Y (2024) Multi-objective optimization of reservoir development strategy with hybrid artificial intelligence method. Expert Systems with Applications 241, 122707.

[DOI: 10.22068/ase.2025.703]

Wang H, Ji C, Shi C, Yang J, Wang S, Ge Y, and Wang X (2023) Multi-objective optimization of a hydrogen-fueled Wankel rotary engine based on machine learning and genetic algorithm. Energy 263, 125961.

Tamashiro K, Omine E, Krishnan N, Mikhaylov A, Hemeida AM, and Senjyu T (2023) Optimal components capacity based multi-objective optimization and optimal scheduling based MPC-optimization algorithm in smart apartment buildings. Energy and Buildings 278, 112616.

Zhou B, Li S, Zi B, Chen B, and Zhu W (2023) Multi-objective optimal design of a cable-driven parallel robot based on an adaptive adjustment inertia weight particle swarm optimization algorithm. Journal of Mechanical Design 145(8), 083301.

Abedzadeh Maafi R, Etemadi Haghighi S, and Mahmoodabadi MJ (2023) Pareto optimal design of a fuzzy adaptive hierarchical sliding-mode controller for an XZ inverted pendulum system. IETE Journal of Research 69(5), 3052-3069.

Kapnopoulos A, and Alexandridis A (2022) A cooperative particle swarm optimization approach for tuning an MPC-based quadrotor trajectory tracking scheme. Aerospace Science and Technology 127, 107725.

Aessa SA, Shneen SW, and Oudah MK (2025) Optimizing PID Controller for Large-Scale MIMO Systems Using Flower Pollination Algorithm. Journal of Robotics and Control (JRC) 6(2), 553-559.

Chen X, Wang Z, Shi H, Jiang N, Zhao S, Qiu Y, and Liu Q (2025) Review of Agricultural Machinery Seat Semi-Active Suspension Systems for Ride Comfort. Machines 13(3), 246.

El-Rifaie AM, Abid S, Ginidi AR, and Shaheen AM (2025) Fractional Order PID Controller Based-Neural Network Algorithm for LFC in Multi-Area Power Systems. Engineering Reports 7(2), e70028.

Sahin AK, Cavdar B, and Ayas MS (2024) An adaptive fractional controller design for automatic voltage regulator system: Sigmoid-based fractional-order PID controller. Neural Computing and Applications 36(23), 14409-14431.

Sadeghian Z, Akbari E, Nematzadeh H, and Motameni H (2025) A review of feature selection methods based on meta-heuristic algorithms. Journal of Experimental & Theoretical Artificial Intelligence 37(1), 1-51.

Slotine JJE, and Li W (1991) Applied nonlinear control 199, 1, 705 Englewood Cliffs, NJ: Prentice hall.

Astrom KJ, Wittenmark B, (2008) Adaptive control, Courier Corporation.

Driankov D, Hellendoorn H, and Reinfrank M (2013) An introduction to fuzzy control. Springer Science & Business Media.

Talatahari S, Azizi M, and Gandomi AH (2021) Material generation algorithm: A novel metaheuristic algorithm for optimization of engineering problems. Processes, 9(5), 859.

Nouhi B, Khodadadi N, Azizi M, Talatahari S, and Gandomi AH (2022) Multi-objective material generation algorithm (MOMGA) for optimization purposes. IEEe Access 10, 107095-107115.

Gheibollahi H, and Masih-Tehrani M (2023) A multi-objective optimization method based on NSGA-II algorithm and entropy weighted TOPSIS for fuzzy active seat suspension of articulated truck semi-trailer. Proceedings of the Institution of Mechanical Engineers, Part C: Journal of Mechanical Engineering Science 237(17), 3809-3826.

Najafi A, Masih-Tehrani M, Emami A, and Esfahanian M (2022) A modern multidimensional fuzzy sliding mode controller for a series active variable geometry suspension. Journal of the Brazilian Society of Mechanical Sciences and Engineering 44(9), 425.

Gheibollahi H, Masih-Tehrani M, and Najafi A (2024) Improving ride comfort approach by fuzzy and genetic-based PID controller in active seat suspension. International Journal of Automation and Control, 18(2), 184-213.

Damavandi AD, Masih-Tehrani M, and Mashadi B (2022) Configuration development and optimization of hydraulically interconnected suspension for handling and ride enhancement. Proceedings of the Institution of Mechanical Engineers, Part D: Journal of Automobile Engineering 236(2-3), 381-394.

Nazemian H, and Masih-Tehrani M (2020) Hybrid fuzzy-PID control development for a truck air suspension system. SAE International Journal of Commercial Vehicles 13(02-13-01-0004), 55-69.

Nazemian H, and Masih-Tehrani M (2020) Development of an optimized game controller for energy saving in a novel interconnected air suspension system. Proceedings of the Institution of Mechanical Engineers, Part D: Journal of Automobile Engineering 234(13), 3068-3080.

Nazemi S, Masih-Tehrani M, and Mollajafari M (2022) GA tuned H∞ roll acceleration controller based on series active variable geometry suspension on rough roads. International Journal of Vehicle Performance 8(2-3), 166-187.

Damavandi AD, Mashadi B, and Masih-Tehrani M (2025) Development of a hybrid intelligent switching hydraulically interconnected suspension system under a multi-objective optimized mode selection strategy with real-world condition. Proceedings of the Institution of Mechanical

[DOI: 10.22068/ase.2025.703]

Engineers, Part D: Journal of Automobile Engineering 239(4), 1222-1239.

Najafi A, and Masih-Tehrani M (2022) Roll stability enhancement in a full dynamic ground-tour vehicle model based on series active variable-geometry suspension. International journal of vehicle performance 8(2-3), 188-223.

Rodriguez-Guevara D, Favela-Contreras A, Beltran-Carbajal F, Sotelo C, and Sotelo D (2023). A differential flatness-based model predictive control strategy for a nonlinear quarter-car active suspension system. Mathematics 11(4), 1067.

[DOI: 10.22068/ase.2025.703]